New Quantum Monte Carlo Method for Determining the Equation of State of One-Dimensional Fermions in Harmonic Traps

Casey Berger

Department of Physics, The Ohio State University, Columbus, OH 43210, USA

(Dated: April 30, 2015)

A Thesis Submitted in Partial Fulfillment of
the Requirements for Graduation with
Research Distinction in Physics

Abstract

The system of interacting, trapped fermions in one dimension has been of interest in both the theoretical and experimental communities. This system is realizable experimentally using ultracold atoms in traps, where the interactions can be tuned to simulate a number of important situations in nuclear theory, condensed matter, quantum information, and QCD. Theoretically, however, this system remains a challenge to treat, and no known benchmarks exist for the ground state energy, Tan's contact, or density profiles for the few- to many-body regime. This project implements a lattice Monte Carlo (LMC) method to solve for these quantities. The method blends hybrid Monte Carlo (HMC) - a pillar of lattice quantum chromodynamics (lattice QCD) - with a non-uniform lattice defined using Gauss-Hermite quadrature points and weights. This coordinate basis is the natural one for the harmonic oscillator trapping potential, and can be generalized to traps of other shapes. Using this method, we determine the ground-state energy and Tan's contact of attractively interacting few-fermion systems in a one-dimensional harmonic trap, for a range of couplings and particle numbers. Complementing those results, we show the corresponding density profiles. We present results for $N = 4, ..., 20$ particles - and the method is capable of extending beyond that. The method is the first lattice calculation of its kind, and is exact up to statistical and systematic uncertainties, which we account for. Our results are therefore a benchmark for other methods and a prediction for ultracold-atom experiments.

Contents

I. INTRODUCTION

A. Context

One-dimensional (1D), *noninteracting* quantum systems in external traps are exactly solvable, and provide a useful exercise for undergraduate quantum mechanics courses. Even for a large number of particles, N, the Hamiltonian can be separated into a sum of the Hamiltonians for each particle, and each Hamiltonian solved in isolation:

$$\hat{H} = \sum_{n=1}^{N} (\hat{T}_n + \hat{V}_{n,ext}), \tag{1}$$

where $\hat{T}_n$ and $\hat{V}_{n,\text{ext}}$ are the kinetic energy and external potential respectively for the nth particle.

Once interactions between particles are turned on, however, this method no longer works, and the Hamiltonian quickly becomes unmanageable. This is the case even for the simple Dirac delta function interaction - with the exception of the two-particle case, discussed further in our results [1]. Once interactions appear in the trapped system, not just in 1D but in all dimensions, numerical methods become necessary.

Not only is it important to use numerical methods, but it is also useful to switch to the formalism of second quantization, where the operators can be written explicitly without reference to the particle numbers. With a few exceptions (discussed later), from this point on, we use second quantization.

The motivation for developing computational methods for low-dimensional quantum systems, in particular many-fermion systems, is manifold. Firstly, these systems have been realized experimentally as quantum wires and as ultracold atomic gases confined in a trapping potential [2],[3],[4]. The latter provide a highly versatile playing field: experimentalists can tune multiple parameters, including temperature, polarization, and strength of the interaction, and therefore study a variety of phenomena, including superfluidity and Bose-Einstein condensation.

Ultracold atomic systems display phenomena that can teach us about the physics of nuclear structure, condensed matter, neutron stars, and more. The reason for this wide versatility is that all these systems display behavior known as "universal" behavior [5],[2],[6]. When the interparticle separation is much larger than the range of the interaction between

the particles and the interparticle separation is much smaller than the scattering length, the system is in the unitary limit. In this limit, the density of the system determines the length scale. This allows the behavior characterised by the system at unitarity to be universal - i.e. unitary systems can occur at any length or energy scale, and indeed we see them in systems with vastly different scaling (for example, in both nuclear and atomic physics, whose length scales differ by a factor of 10^5).

In addition, low-dimensional systems display physics that is often non-perturbative and not easily captured by mean-field analyses, which means computational methods are necessary [7]. However, the associated computational cost is considerably lower than for their higher dimensional counterparts, which makes them ideal for testing computational many-body physics.

Spatially homogenous many-fermion systems with contact interactions can be solved exactly in one spatial dimension (1D) via the Bethe Ansatz [8][2], but this approach is not helpful when fermions are confined by an external trap (such as a harmonic oscillator potential), as introducing an external potential breaks the translational symmetry of the homogenous case. Similarly, in higher dimensions such exact solutions are generally unavailable; this makes quantum Monte Carlo (QMC) methods valuable. Of the large array of QMC methods available, we focus on a lattice-based approach, as we intend to benefit from hybrid Monte Carlo (HMC), which is one of the pillars of lattice QCD, and an essential component for three -dimensional (3D) studies, to which we aspire to extend this method.

Many-body methods, in particular HMC, rely heavily on linear-algebra operations such as matrix-matrix and matrix-vector multiplication. In uniform systems with periodic boundary conditions, these matrices have a structure which enables the use of Fourier acceleration techniques, namely the fast Fourier transform (FFT), in particular via FFTW [9]. Including trapping potentials, however, breaks the symmetry and changes the boundary conditions, and thus spoils the use of such acceleration techniques. Progress in the mid-1990's in the context of fast polynomial transforms resulted in libraries that solve this problem, namely NFFT [10], which allow for fast transforms in non-uniform lattices. The approach used here benefits from these developments.

This project presents a new method of determining important properties of an interacting system of two-component spin fermions in one dimension, confined in a harmonic oscillator (HO) potential. Work began in May of 2014 as part of the Computational Astronomy and

Physics Research Experience for Undergraduates (CAP REU) at the University of North Carolina at Chapel Hill (UNC-CH). This project was supervised by Dr. Joaquín Drut at UNC-CH and performed in collaboration with Dr. Drut and with Dr. Eric Anderson, also at UNC-CH. Dr. Richard Furnstahl at the Ohio State University (OSU) advised and supervised the thesis process.

B. Literature Review

Our understanding of the quantum mechanics of many-particle systems is undergoing a remarkable transformation, both in theory and experiment. On the theoretical side, quantum-information concepts are being actively studied as a new way to understand quantum mechanics, in particular quantum phase transitions [8]. Simultaneously, computational methods to tackle these problems have made great advances, fueled by efforts from the condensed matter, materials science, and lattice quantum chromodynamics (QCD) communities. On the experimental side, our ability to manipulate ultracold quantum gases continues to make great strides [2],[3],[4]. It is now possible to experimentally simulate simple (yet useful) systems relevant for condensed matter, atomic and nuclear physics, and progress is being made towards more complex degrees of freedom.

Recent experiments on ultracold atomic gases in one dimension have given us a better understanding of quantum many-body systems. These atoms are restricted to move in one dimension by tightly confining them in the two transverse directions, but only weakly longitudinally [2]. In other words, the frequency of the harmonic trap is very large in the two transverse directions, which makes the energy gap between the ground state energy and the first excited state large enough that it becomes virtually inaccessible (i.e. it would take an extremely high energy for the atoms to escape the ground state in all but the longitudinal direction).

Ultracold atomic systems are ideal for modeling a wide range of phenomena due to the precision with which they can be controlled and manipulated. In particular, strongly interacting fermions can be studied. These systems can be found in a large variety of areas in physics: for example, inside a neutron star, in atomic nuclei, in the quark-gluon plasma of the early Universe, and in strongly correlated electron systems [3],[4].

Treating this system theoretically, however, remains a challenge. In one dimension, the

spatially homogenous system with contact interactions can be solved analytically using the Bethe Ansatz. The Bethe Ansatz is a particular form of wave function which solves for the energy eigenspectrum exactly [2]. However, once a trapping potential is introduced, the Bethe Ansatz wave function is no longer an eigenfunction of the Hamiltonian.

A typical way to address the challenge introduced by the trapping potential consists in first solving the homogeneous problem and then using the local-density approximation (LDA). The LDA assumes that each point in space can be considered as a uniform system, with energy density $\epsilon(\rho)$ evaluated at the local density $\rho(r)$ in the trapped system [11],[12]

$$E^{LDA}[\rho] = \int \epsilon[\rho(r)] d^3\mathbf{r} \tag{2}$$

shown here in the general, 3D case.

This approximation fails at the edges of the trap, however, introducing uncontrolled errors in the calculation. Therefore, a direct non-perturbative calculation of the energy in a trap is highly desirable. Such a calculation can be achieved using exact diagonalization, but exact diagonalization methods are limited to few-particle systems [13].

Due to the challenges that this system presents, there are no known benchmarks for many quantities of this system that are of interest in both theory and experiment. Our method proposes to solve this system exactly - with controlled numerical errors - and compute the energy, Tan's contact([14],[15],[16]), and density profiles for the system at zero temperature and for a range of particle numbers covering the transition from few- to many-body.

C. Monte Carlo Methods and the Ising Model

The goal of many-body lattice methods is to develop expressions that allow us to evaluate operators stochastically. The end result is a method that calculates the observables exactly, up to statistical and systematic errors due to the finite size and lattice spacing (which can be quantified) [7]. The exact result for the expectation value of an observable, $\hat{\mathcal{O}}$, can be given by

$$\langle \hat{\mathcal{O}} \rangle = \frac{1}{\mathcal{Z}} \sum_n \mathcal{P}_n \mathcal{O}_n \tag{3}$$

where $\mathcal{P}_n$ is a positive semi-definite probability measure determined by the problem, and $\mathcal{Z} = \sum_n \mathcal{P}_n$. The index n parameterizes a set of auxiliary variables (for example the auxiliary

fields used to represent a two-body interaction in a Hubbard-Stratonovich transformation). These variables are distributed according to $\mathcal{P}_n$.

The sum is performed using Monte Carlo methods, such that:

$$\langle \hat{\mathcal{O}} \rangle \simeq \frac{1}{N_s} \sum_{n=1}^{N_s} \mathcal{O}_n, \tag{4}$$

where N_s is the number of samples of auxiliary variables, and $\mathcal{O}_n$ is the expecation value of the operator $\hat{\mathcal{O}}$ in the n-th case. If the N_s samples are uncorrelated, then the uncertainty on this approximation is $\sqrt{\sigma^2/N_s}$, where σ is the standard deviation.

For the zero-temperature case (which is the one we examine in this project), the partition function can be defined as

$$\mathcal{Z} = \langle \psi_0 | e^{-\beta \hat{H}} | \psi_0 \rangle, \tag{5}$$

where $\beta = 1/(k_B T)$. The Hamiltonian, $\hat{H}$ is defined (in second quantization) as

$$\hat{H} = h^{(1)}_{\alpha\beta} \hat{a}^\dagger_\alpha \hat{a}_\beta + h^{(2)}_{\alpha\beta\gamma\delta} \hat{a}^\dagger_\alpha \hat{a}^\dagger_\beta \hat{a}_\gamma \hat{a}_\delta + h^{(3)}_{\alpha\beta\gamma\delta\mu\nu} \hat{a}^\dagger_\alpha \hat{a}^\dagger_\beta \hat{a}^\dagger_\gamma \hat{a}_\delta \hat{a}_\mu \hat{a}_\nu + ... \tag{6}$$

This is a general Hamiltonian, including terms for one-, two-, three-, and higher-body forces. The particle number operator is defined as

$$\hat{N} = \sum_\alpha \hat{a}^\dagger_\alpha \hat{a}_\alpha. \tag{7}$$

Next, we can represent the partition function through fields, such that

$$\mathcal{Z} = \int \mathcal{D}\psi^\dagger \mathcal{D}\psi e^{-S[\psi^\dagger, \psi]}. \tag{8}$$

Now that the partition function is defined via fields, we can put those fields on a lattice. We discretize spacetime into $N_x \times N_\tau$ points and define fields on this $1+1$ dimensional lattice.

Once we have our system represented on a lattice, we can use Monte Carlo methods to sample configurations of the lattice and take averages to compute the observables. One of the most popular methods used to tackle lattice-based quantum problems is called Markov-chain Monte Carlo (MCMC) - based on the Metropolis algorithm.

Central to the MCMC method is the partition function of a system and the probability distribution. For an example, the Ising Model is used here. Recreation of the Ising Model was used as a warm-up project at the start of this thesis work, in order to gain experience with and understanding of Monte Carlo methods.

The Ising Model is a model of a ferromagnet, which uses MCMC to determine the observables of the system, such as the energy and the magnetisation, at various temperatures [17],[18]. In the case of the 2D Ising model, the system can be represented relatively simply as spins on an $L \times L$ lattice. The number of spins on the lattices is $N = L \times L$, and the size of the configuration space (i.e. possible number of configurations of the lattice) is 2^N.

The Hamiltonian for a specific spin in the Ising model is

$$H_i = -J \sum_{<i,j>} s_i s_j \tag{9}$$

where J is the strength of the coupling between nearest neighbor spins, and $< i, j >$ indicates that the sum is done over the nearest neighbors, j, of spin site i. Periodic boundary conditions are imposed, meaning that the top-most spins on the finite lattice "see" the bottom-most spins as their neighbors and vice versa, and the left-most spins "see" the right-most spins as their neighbors (and again vice versa). Topologically, this forms a torus, the 2D surface of which is our lattice.

The normalized Boltzmann distribution of the system gives the probability that the system will be in a particular configuration, and is expressed as

$$\mathcal{P}(\alpha) = \frac{1}{\mathcal{Z}} e^{-\beta E(\alpha)} \tag{10}$$

where α is the configuration and $E(\alpha)$ is the energy of the system with that configuration. The observables of interest in the Ising model - the magnetization, M, and the energy, E - can both be found using probability summing:

$$\langle M \rangle = \sum_{\alpha} M(\alpha)\mathcal{P}(\alpha), \tag{11}$$

and

$$\langle E \rangle = \sum_{\alpha} E(\alpha)\mathcal{P}(\alpha). \tag{12}$$

This may appear simple, but as we have already seen, the size of our configuration space (or the number of total configurations, α, that we would have to sum over to get the solution exactly) is 2^N. For a 2×2 lattice, this could be done quickly. But if we want to approximate real systems (i.e. approach the thermodynamic limit), we need to use much larger lattices. Even for the relatively small lattice size of 10×10, the sum would need to be performed over roughly 10^{30} configurations.

In order to perform a sum over a much smaller number of configurations and retain accuracy, Monte Carlo methods are used to generate a representative sample of configurations. Monte Carlo methods are by definition stochastic methods, which use a random number generator and evolution of the system over time to generate this representative sample. In practice, we use the Metropolis Algorithm. The process begins with a lattice initialized with a random configuration of spins, determined using a random number generator and a binary selection process. The initial energy is calculated, using the equation

$$E(\alpha) = -\frac{1}{2}J \sum_{i=1,<i,j>}^{N} s_i s_j, \tag{13}$$

where α is the configuration. Then, a point on the lattice is selected (again, randomly, using our random number generator), and the spin is flipped. The energy of this new configuration is computed using Eq. 13, and the change in energy, ΔE between the new configuration and the previous configuration is found.

This configuration is then checked in the following way: since every energy comes with a probability, $\mathcal{P}(\alpha)$, determined in Eq. 10 and using ΔE as our energy, we are able to select samples based on the probability that they would occur. Using a random number generator, we select a value in the range $0.0 - 1.0$ and then compare it to the ratio of the probability distributions, $\mathcal{P}(\alpha)$, of the configurations before and after the flip. If the random number is higher than the ratio of the probability, that sample is rejected, the spin is flipped back, and a new site is selected.

This process is repeated for few sweeps over the lattice initially without saving any of the configurations. This is the thermalization process. After the lattice has equilibrated, the algorithm continues the process, this time saving the configuration and energy of the configuration. At the end, the saved energy values were averaged for each temperature step.

The end result is a representative sample of the configurations, based on the statistical probability that the energy of the configurations sampled would occur. This allows for a much smaller number of samples which still reproduce the observables. An example of the data from a 2D Ising Model compared with the known analytical solution for the 2D ferromagnet are included in Appendix G.

II. METHODS AND OBJECTIVES

This project focused on a system of one-dimensional spin-1/2 fermions in an external trap, such that

$$\hat{H} = \hat{T} + \hat{V}_{\text{ext}} + \hat{V}_{\text{int}}, \tag{14}$$

where $\hat{T}$ is the kinetic energy operator corresponding to a non-relativistic dispersion relation $E = p^2/2m$; $\hat{V}_{ext}$ is the external harmonic trap of frequency ω, and $\hat{V}_{\text{int}}$ is the two-body attractive zero-range interaction characterized by a bare coupling g.

To account for the external harmonic-oscillator (HO) trap directly, we implement the novel feature of a non-uniform spatial lattice. In particular, we choose the Gauss-Hermite (GH) integration points and weights. The Gauss-Hermite polynomials are the natural basis for the HO system - the Hermite polynomials times a Gaussian are the solution to the Schrödinger equation for a particle trapped in a harmonic potential well.

For reference, in Fig. 1 we plot the GH abscissas and weights for the main lattice sizes used in this work. With this basis, we are able to combine $\hat{T}$ and $\hat{V}_{\text{ext}}$, such that the sum

$$\hat{T} + \hat{V}_{\text{ext}} = \sum_k \hbar\omega_k \hat{n}_k, \tag{15}$$

where $\hbar\omega_k = \hbar\omega(k + 1/2)$, has a diagonal form in the HO basis. This takes advantage of our GH lattice. Here, the operator $\hat{n}_k = \hat{n}_{\uparrow,k} + \hat{n}_{\downarrow,k}$ counts the number of HO excitations in level k of both spins.

On the GH lattice, the integral over a given function $f(x)$ is approximated by

$$\int dx\ e^{-x^2} f(x) \simeq \sum_{i=1}^{N_x} w_i\ f(x_i), \tag{16}$$

where the abscissas x_i are given by the roots of the Hermite polynomial of degree N_x, and w_i are the (positive) weights given by

$$w_i = \frac{1}{H_{N_x-1}(x_i) H'_{N_x}(x_i)}, \tag{17}$$

where $H_n(x)$ is the Hermite polynomial of order n [19].

The $2N_x$ variables $\{x_i, w_i\}$ take the above form when chosen such that the integral in Eq. 16 is represented *exactly* by the sum on the right and when $f(x)$ is a polynomial of degree $\leq 2N_x - 1$. This choice ensures that the Hermite polynomials form an (exactly)

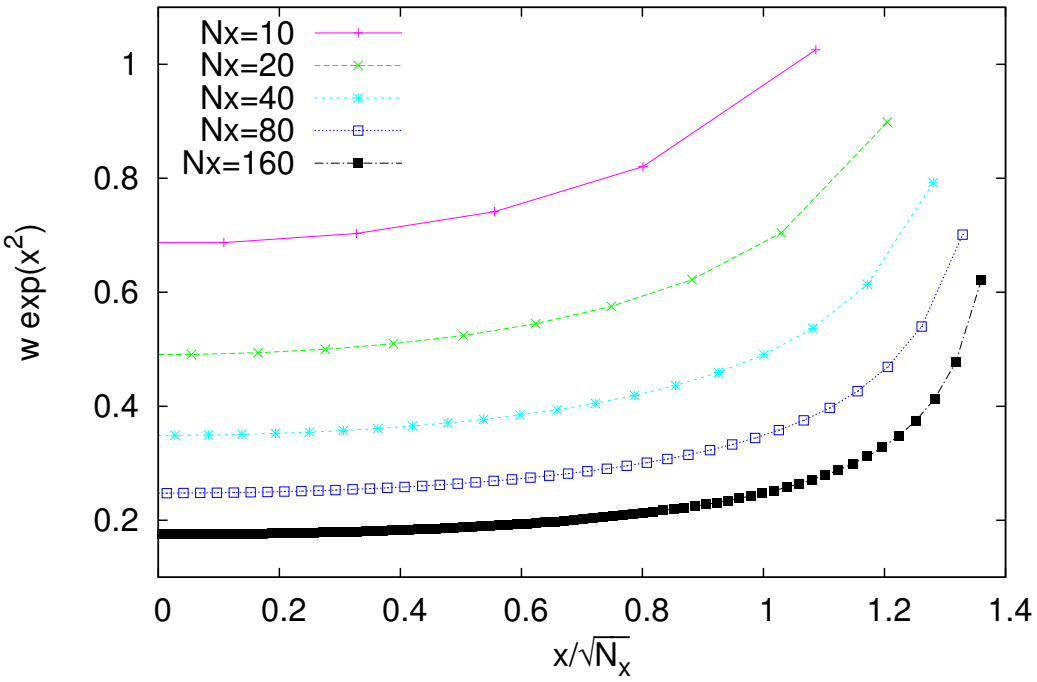

FIG. 1: Abscissas and weights for Gauss-Hermite integration with $N_x = 10, 20, 40, 80, 160$ points. The x axis is scaled by $1/\sqrt{N_x}$ for display purposes.

orthogonal set when evaluated on the $\{x_i\}$ lattice (relative to a scalar product defined with the w_i weights).

For this property to hold with the same accuracy on a uniform lattice, a larger number of points would be needed. Thus, our choice preserves both the orthogonality *and* the dimensionality of the coordinate representation as the spatial dual of an HO basis of size N_x, which therefore allows for a precise representation of HO wavefunctions up to $k = N_x - 1$ in Eq. 15. It is worth noting that the same approach can be pursued for other types of external potentials; for instance, for a triangular external potential $v(x) \propto |x|$ one would use the so-called Airy functions, and associated points and weights. The Airy functions are the solution to the Schrödinger equation when the trapping potential is a triangular well.

The interaction potential introduced in this system is a contact interaction (which in first quantization is represented as a delta function $\delta(r_1 - r_2)$), as

$$\hat{V}_{\rm int} = -\, g \sum_i \hat{n}_{\uparrow i}\, \hat{n}_{\downarrow i}, \tag{18}$$

Using the GH lattice, the discretized interaction becomes

$$\hat{V}_{\text{int}} = -\, g \sum_{i=1}^{N_x} w_i e^{x_i^2}\ \hat{n}_{\uparrow i}\, \hat{n}_{\downarrow i}, \tag{19}$$

where $\hat{n}_{\lambda i}$ is the lattice density operator for spin λ at position i. Thus, we obtain a position-dependent coupling constant $g(x_i) = g\, w_i e^{x_i^2}$ (see Fig. 1).

In order to be able to treat the interaction potential in the Hamiltonian of this system, we use a Hubbard-Stratonovich (HS) transformation, discussed further in Appendix D. The Hubbard-Stratonovich transformation casts the two-body interaction as a sum over one-body operators, which appear as external auxiliary fields [7].

We place the system in a (GH discretized) spatial lattice with N_x points, and approximate the Boltzmann weight via a symmetric Suzuki-Trotter decomposition, discussed more in Appendix C:

$$e^{-\tau \hat{H}} = e^{-\tau/2(\hat{T}+\hat{V}_{\text{ext}})} e^{-\tau \hat{V}_{\text{int}}} e^{-\tau/2(\hat{T}+\hat{V}_{\text{ext}})} + \mathcal{O}(\tau^3), \tag{20}$$

for some small temporal discretization parameter τ. This discretization of imaginary time results in a temporal lattice of extent N_τ, which we also refer to below in terms of $\beta = \tau N_\tau$ and in dimensionless form as $\beta\omega$. Note that throughout this work, we use units such that $\hbar = m = k_B = \omega = 1$, where m is the mass of the fermions and ω is the frequency of the harmonic trap. These are our fundamental units, or "lattice units." As our spatial lattice is non-uniform, the abscissas are in lattice units, and our temporal lattice is discretized as $\tau = 0.05$ in lattice units.

The projection Monte Carlo method, further discussed in Appendix E, is used to isolate the ground state and its corresponding energy. The projection Monte Carlo method applies a filter, in the form of the operator: $e^{-\beta \hat{H}}$ to separate the ground state and suppress higher energy states. However, for systems which converge quickly to the ground state, the projection Monte Carlo method can amplify the noise. To avoid the problem of introducing noise, the range of β was limited and the ground state energy extrapolated by fitting the data to an exponential, as in Fig. 2

In the homogenous case, it is common in Monte Carlo calculations to switch between coordinate and momentum space in order to take advantage of Fourier acceleration techniques via fast Fourier transform (FFT) algorithms. The interaction term - $\hat{V}_{\text{int}}$ - of the Hamiltonian can be most easily evaluated in coordinate space, and the kinetic term - $\hat{T}$ -

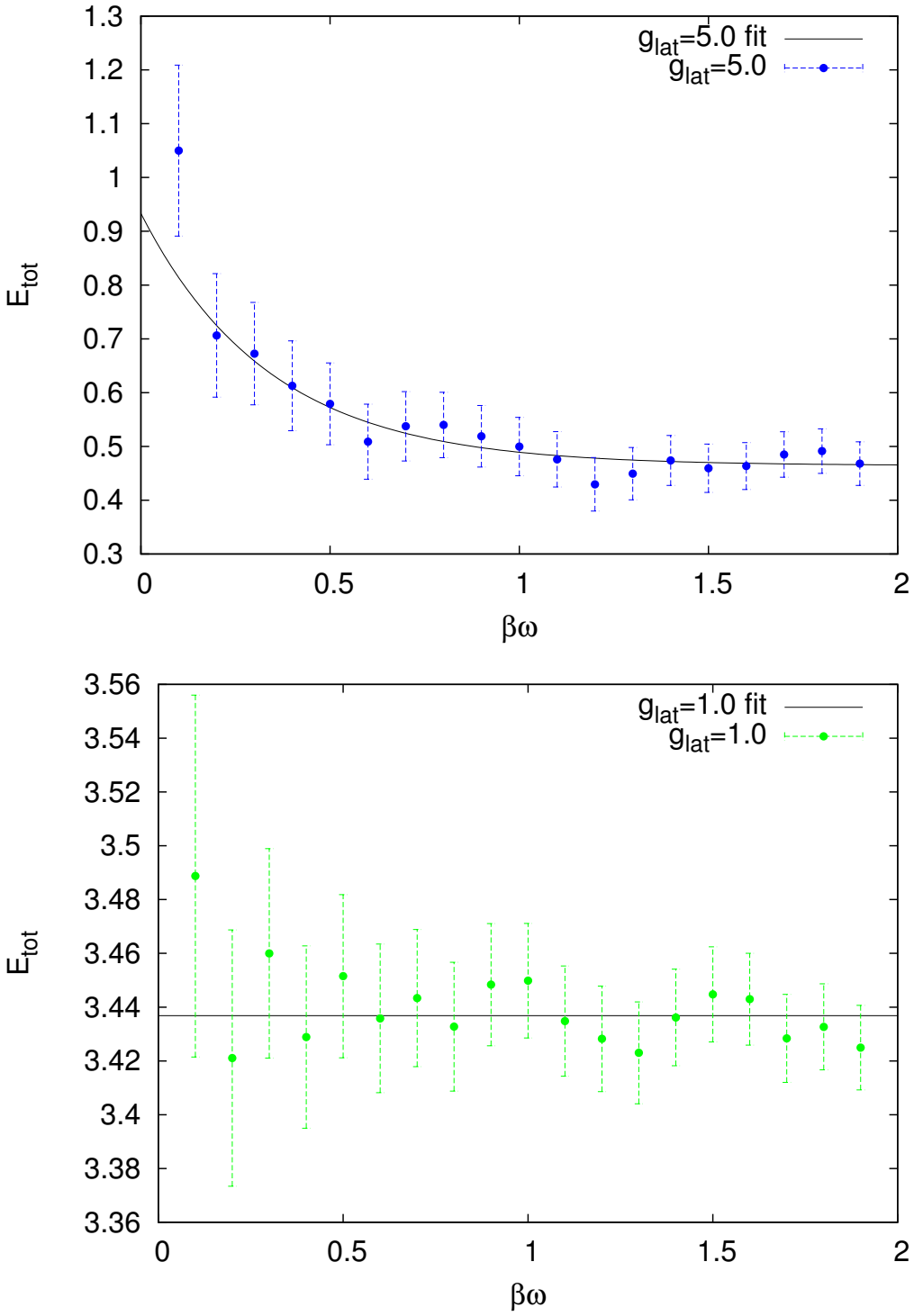

FIG. 2: Top: The solid line shows fit to an exponential $A + Be^{-\beta\omega/C}$, in order to extrapolate the ground state energy. Bottom: The solid line here shows a fit to a constant, as the system converged quickly to the ground state.

in momentum space. In the present approach, instead, we switch between coordinate and HO space, implementing the imaginary-time evolution by applying the $\hat{T} + \hat{V}_{\text{ext}}$ piece in HO space, and the $\hat{V}_{\text{int}}$ piece in coordinate space.

Our approach utilizes the HMC method, which is chiefly a lattice QCD technique but which we have adapted to our non-relativistic system. Hybrid Monte Carlo is a blend of Markov-chain Monte Carlo (MCMC) and molecular dynamics [7]. It implements a Hamiltonian evolution between samples by introducing a fictitious momentum that is conjugate to the auxiliary field that represents the interaction. This enables global lattice changes, further decreasing the time required to account for quantum fluctuations. HMC is discussed in greater detail in Appendix F.

While previous methods have used HMC to greatly increase efficiency and decrease computing time, the introduction of a non-uniform lattice is a novel approach to solving a many-fermion system in a harmonic oscillator trap. Common techniques that implement Monte Carlo methods consist of particles in a uniformly-spaced lattice, but most natural systems are non-uniform. This non-uniform lattice reproduces the trapping potential exactly. In addition, this formulation bypasses the problem of dealing with periodic boundary conditions, which are problematic for trapped systems as they introduce spurious copies of the system across the boundaries. This method is unique because it accounts for such features by also combining HMC with a non-uniform lattice for the first time.

The acceleration in non-uniform lattices of N points yields $O(N \log^2 N)$ operations, rather than the naive $O(N^2)$ operations required for matrix vector multiplication. This is not as advantageous as the FFT-based acceleration in uniform lattices (which yields $O(N \log N)$ operations), but it is a remarkable gain which becomes crucial in high-dimensional systems, as $N = L^d$, where L is the side length of the lattice and d the dimensionality of the problem. With current hardware, this acceleration is not essential for 1D systems, but it is crucial in 3D.

III. RESULTS

A. Zero Coupling Case (Free Gas Test)

The case of non-interacting fermions in a harmonic trapping potential has an exact, analytical solution which is easy to compute. In the ground state, one fermion of each flavor occupies the lowest energy state of each harmonic trap. Since we are in the noninteracting case, we will again use first quantization, in order to show that the Hamiltonian is a sum over all the single-particle Hamiltonians:

$$\hat{H} = \sum_n \left(\frac{\hat{p}_n^2}{2mn} + \frac{1}{2}\omega^2 m \hat{x}_n^2 \right) \tag{21}$$

By solving Schrödinger's equation, the exact solution can be obtained (see Appendix A). The Hamiltonian is a sum over independent particles, so Schrödinger's equation can be separated into independent equations and solved for each particle.

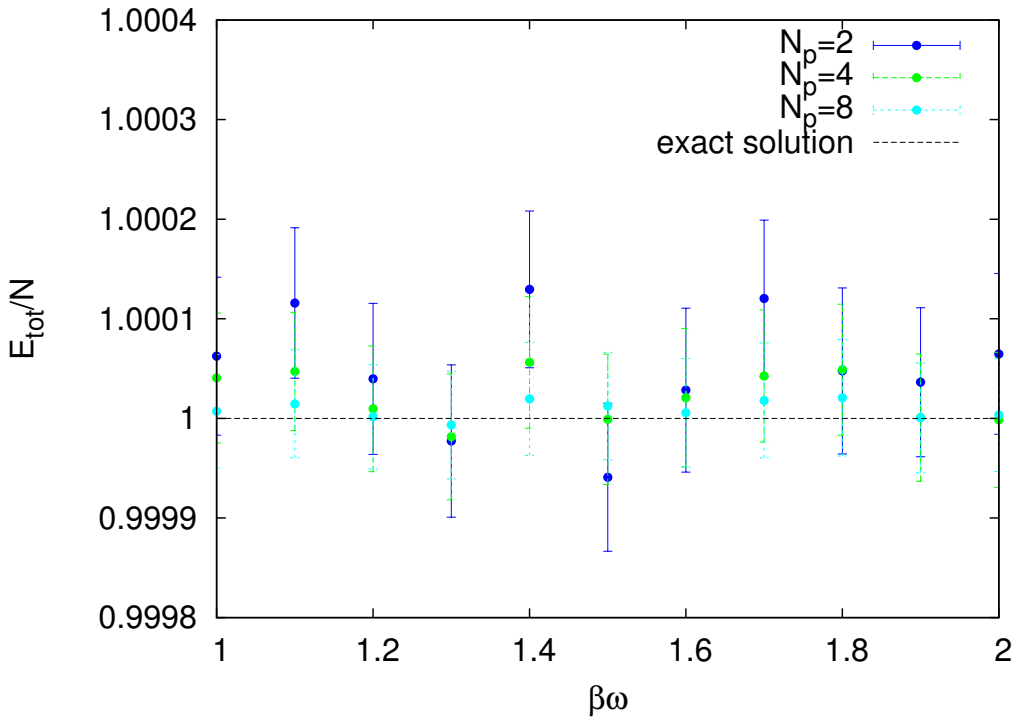

FIG. 3: Results for free gas ($g = 10^{-6}$), shown with exact solution for zero coupling. The energy is scaled by number of particles.

The results of the program compared with the exact solution is shown in Fig. 3 for the case of two, four, and eight pairs of particles.

Some amount of noise can be seen in the figure. Part of this is due to limitations which prevent us from calculating the observables with a truly zero coupling. In the calculation of the observables, we divide through by the coupling, resulting in a value that diverges. Instead, we calculate the observables with a negligible coupling on the order of 10^{-6}. We normalized our data by dividing by the predicted value of the ground state energy (the exact solution).

B. The Two-Body Problem

Another exact, analytical solution that is available to us in 1D is the two-body case: two particles with opposite spin with a delta function interaction. The case of one pair of particles with opposite spin was examined and results compared with the known, exact solution (see Fig. 4). For one pair of particles, various couplings between the particles were examined.

The exact solution for a pair of particles with opposite spin confined in one dimension by a harmonic oscillator trap is obtained by solving the Schrödinger equation for the following Hamiltonian (again in first quantization, as it is only a two-particle problem):

$$\hat{H} = \frac{\hat{p}_1^2}{2m} + \frac{1}{2}k\hat{x}_1^2 + \frac{\hat{p}_2^2}{2m} + \frac{1}{2}k_2\hat{x}_2^2 + g\delta(\hat{x}_1 - \hat{x}_2) \tag{22}$$

The ground state energy for this case at varying couplings using our method is shown in Fig. 4, alongside the exact solution [1]. It can be seen that, while our data lies on a similar curve, that curve does not naively match the exact solution. In fact, the use of a non-uniform lattice introduces a need for a renormalization factor when varying the interaction coupling.

In a uniform basis, certain physics parameters such as the scattering length are fixed; however, this method implements a non-uniform basis, in which not only the size of the lattice but also the density of the lattice sites is altered with different lattice sizes. A renormalization factor on the varied parameter (i.e. the coupling of the system) which is proportional to the size of the lattice must be included to maintain constant physics between bases.

To tune the system to a specific physical point, determined by the 1D scattering length a_0 in units of the HO length scale $a_{\mathrm{HO}}(= 1$ in our units), we computed the ground-state energy of the two-body problem and matched it to that of the continuum solution (see e.g. [1]).

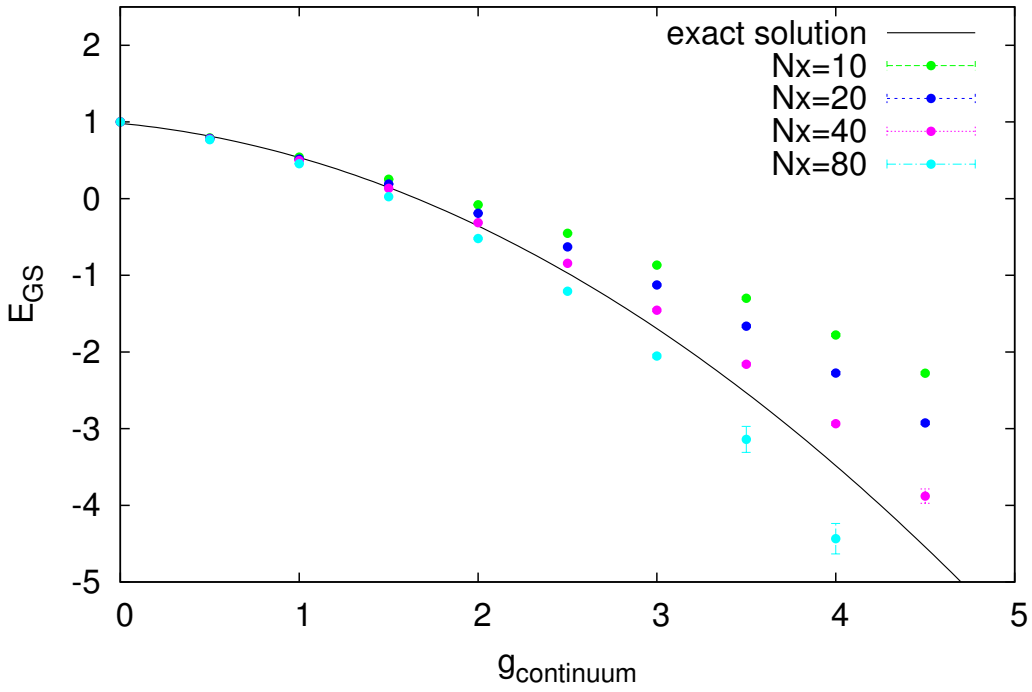

FIG. 4: Results for the two-body case on different lattice sizes, shown with exact solution.

Once the coupling constant was determined, and the two-body physics thus fixed, we varied the particle number and computed other observables.

C. The Ground State Energy

In this section we show our results for the ground-state energy $E_{\rm GS}$ for a variety of particle numbers and couplings. To find $E_{\rm GS}$ we calculated the $\beta\omega$-dependence of the expectation value of the Hamiltonian $\langle\hat{H}\rangle$ and extrapolated to large $\beta\omega$ (see discussion under Eq. 20), as shown in Fig. 5.

The Monte Carlo estimates of $\langle\hat{H}\rangle$ were obtained by averaging over 10^4 de-correlated samples, which ensured a statistical uncertainty of order 1%. Conventional extrapolations would include an exponential decay to a constant value, but for the systems studied the exponential fall-off was sufficiently negligible to allow for a simple fit to a constant (as discussed in Fig. 2). Because 15-20 points in total were used for the $\beta\omega$ fits, the above statistical effects translated into error bars in $E_{\rm GS}$ on the order of 1% or better at weak coupling, but as large as 5% at the strongest couplings.

The oscillations at the strongest coupling in Fig. 5 are evidence of one of the difficulties

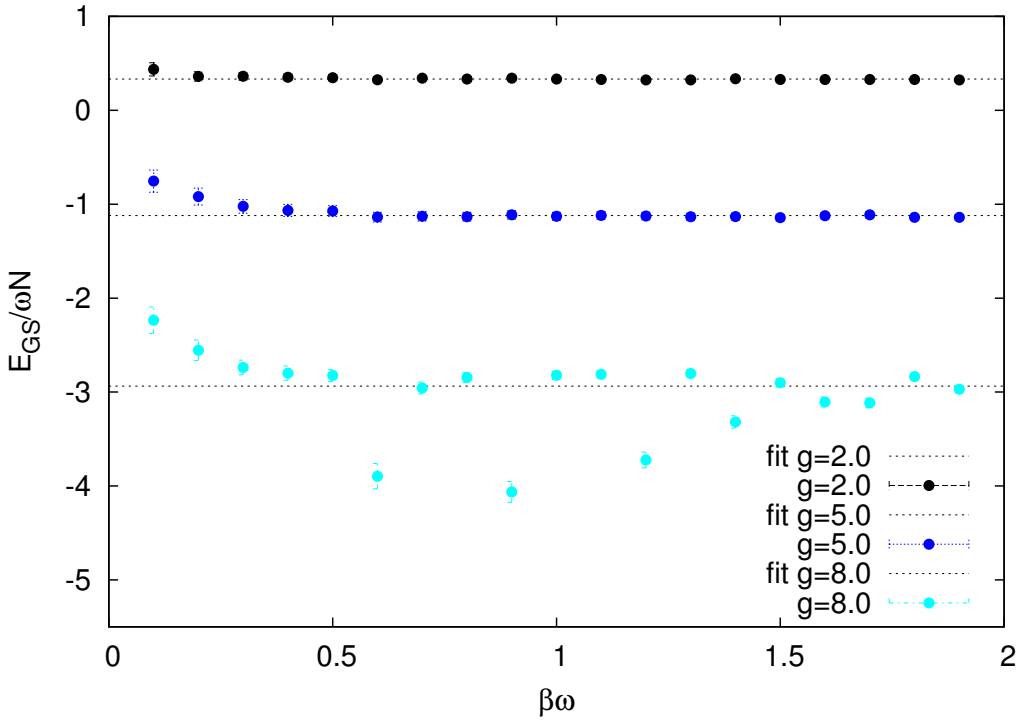

FIG. 5: Large-$\beta\omega$ extrapolation for the energy of 4 particles on a lattice of $N_x = 10$ points. The oscillations in the data at the largest coupling exemplifies the numerical difficulties of computing in that regime.

encountered in computing observables in the strongly coupled regime. The random walks in the HMC algorithm occasionally get "stuck," and the acceptance rate for that particular value of $\beta\omega$ fall far below 1.0. In those cases, we leave the "stuck" points out of our fit when we extrapolate to the ground state.

In Fig. 6 we show our results for the ground-state energy per particle of 4, 6, 8, 10, 12, 16 and 20 particles, in units of $\hbar\omega$. As evident in the figure, systematic finite-size effects are very small for 4, 6 and 8 particles, and only become visible for the smallest lattice size ($N_x = 10$) and for the highest particle numbers. The results otherwise collapse to universal curves that depend only on $a_{\rm HO}/a_0$ and N, showing that the renormalization procedure works as expected. This property must hold if our method is valid, as it indicates that we correctly approach the continuum limit.

As the number of particles in the system approaches infinity, we expect to see convergence to the thermodynamic limit. To see this, we normalized the ground state energy to units of the free gas ground state. The results are plotted in Fig. 7. In the top figure, we can

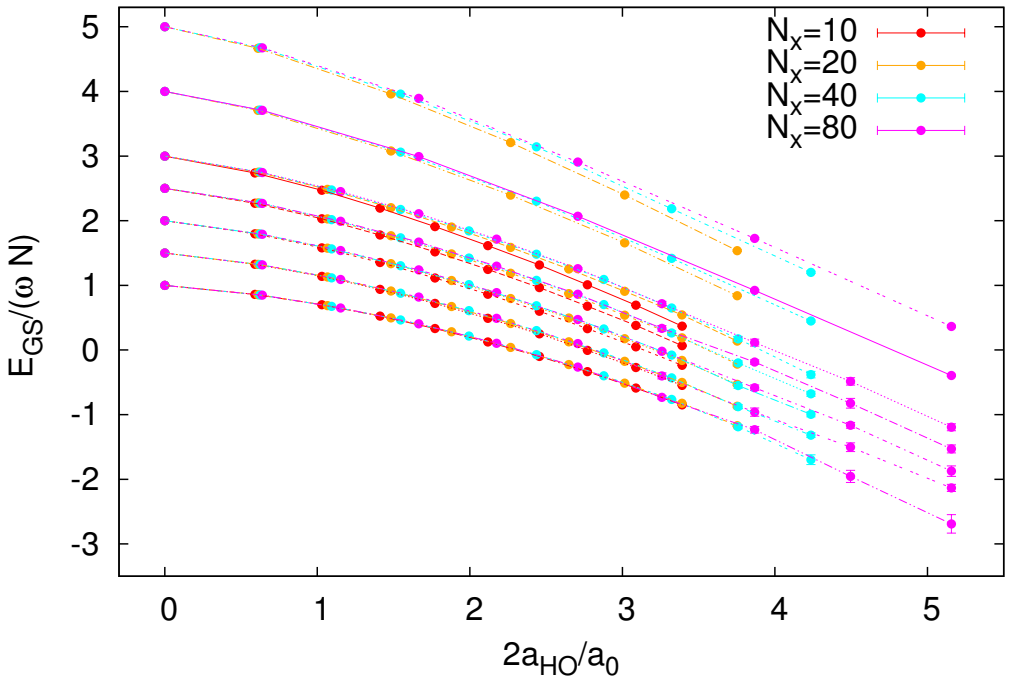

FIG. 6: Ground state energies per particle for N =4, 6, 8, 10, 12, 16, and 20 particles (from bottom to top) as a function of the coupling for lattices of N_x = 10, 20, 40, and 80 points.

see that as the number of particles increases, the amount that the energy changes becomes smaller and smaller. This is evidence of convergence to the thermodynamic limit, and can be seen more easily in the bottom figure of Fig. 7, where we extrapolate to $N \to \infty$.

D. Tan's Contact

For systems with short-range interactions, Shina Tan showed that all the short-range correlations are contained in one quantity, called the contact, $\mathcal{C}$ [14],[15],[16]. The momentum distribution of a two-component Fermi gas with a large scattering length has a tail that falls off as $\mathcal{C}/k^4$, for large k [14],[15], and Tan showed that the energy of the system can be directly related to the momentum distribution, and this relationship is independent of all the details of the short-range interaction with the exception of the scattering length, a:

$$E_{internal} = \frac{V\mathcal{C}}{4\pi a m} + \lim_{K\to\infty} \sum_{k<K,\sigma} \frac{k^2}{2m}(n_{k,\sigma} - \frac{\mathcal{C}}{k^4}), \tag{23}$$

where V is the volume of the system, and $n_{k,\sigma}$ is a fermion with momentum k and spin σ. This relation is true for any finite energy of the system, regardless of number of fermions,

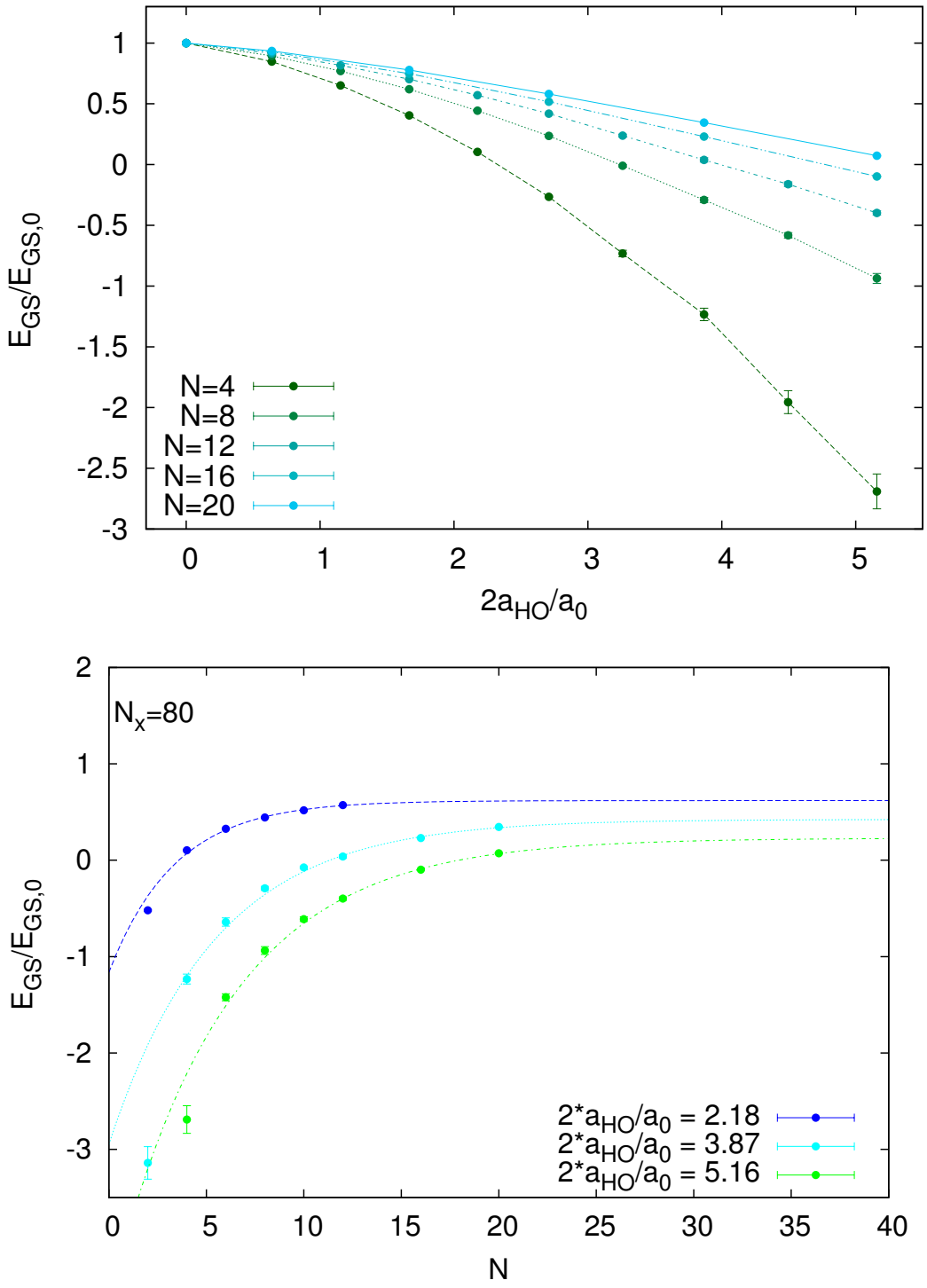

FIG. 7: Top: Ground state energy E_{GS} in units of the non-interacting ground state energy, $E_{GS,0}$ for N =4, 8, 12, 16, 20 particles, showing the approach to the thermodynamic limit, $N \to \infty$. Bottom: Extrapolations to $N \to \infty$ for three different couplings on a lattice of $N_x = 80$.

temperature of the system, polarization, or state [15].

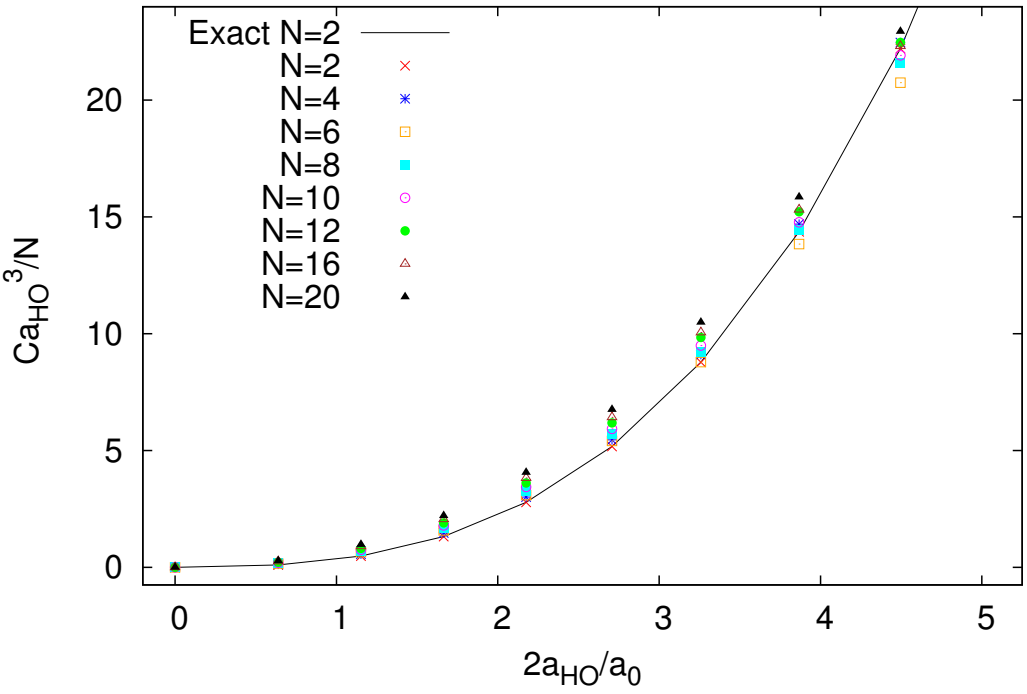

FIG. 8: Contact per particle for 2, 4, 6, 8, 10, 12, 16 and 20 particles, as a function of the coupling, for $N_x = 80$. For 2 particles the exact solution is also shown as a solid line.

Tan's contact can be calculated by taking a derivative of the ground state energy, E_{GS}, with respect to the scattering length. This can be rewritten in terms of the coupling, as

$$\mathcal{C} = 2\frac{\partial E_{\rm GS}}{\partial a_0} = -\frac{1}{a_{\rm HO}}\left(\frac{2a_{\rm HO}}{a_0}\right)^2 \frac{\partial E_{\rm GS}}{\partial(2a_{\rm HO}/a_0)}, \tag{24}$$

which allows us to compute $\mathcal{C}$, using the energy and coupling data we have already shown. Our results for the contact (per particle), for $N_x = 80$, are shown in Fig. 8, along with the known solution for the 2-body case. For the couplings used, the contact per particle shows essentially no dependence on the particle number, which indicates that the thermodynamic limit is reached quickly in these systems.

E. Density Profiles

While the ground state energy and the contact are quantities that are valuable for theory, and are easy to check against our benchmark, the density profile is a quantity which is of

particular interest in experiment. Experiments in ultracold atomic physics can determine the densities of the systems via a number of methods (see e.g. Refs. [3],[4]), thus making a benchmark like the one demonstrated here of great value [2]. This quantity is also of interest to theory, as the most common approach to solving the trapped, interacting one-dimensional system is to combine the Bethe Ansatz with the local density approximation, which introduces uncontrolled approximations.

We attempt here to overcome this limitation by presenting density profiles of the system. All density profiles shown here correspond to the lattice of $N_x = 80$ sites and are normalized to the number of particle pairs ($N/2$). We averaged over 10^4 density samples for each profile.

In Fig. 9 we show the density profiles for several particle numbers $N = 4, 8, 12, 16, 20$. For reference, we provide the result for the non-interacting case, followed by an intermediate coupling, and a strong coupling. The attractive interaction compresses the profile, peaking the oscillations more sharply as the strength of the interaction coupling increases.

In Fig. 10, we show the density profiles for fixed particle numbers. Here, the compression of the oscillations is more clear. As a check on the validity of these density profiles, the area beneath the curve was integrated. Since the curves were normalized to the number of pairs of spin up and spin down fermions, integrating over the entire area should give back $N/2$. The integration was performed numerically, using the Gauss-Hermite points and weights, and the density profiles were found to accurately reproduce the number of pairs.

It is interesting to note the relatively limited interaction dependence of the density profiles, as well as the appearance of oscillations. It is also interesting to note that the number of density oscillation peaks is one half the number of particles. Particles of opposite spin tend to pair up to minimize the energy, and tend to separate from other pairs due to the Pauli principle. This repulsive effect, along with the short range nature of the interaction, minimizes the change in the width of the density profiles with increasing coupling.

IV. ERROR ANALYSIS

This section elaborates on some of the systematic effects in our calculations, namely the dependence of the ground-state energy with the number of spatial lattice sites and the temporal lattice spacing.

In numerical methods on a lattice, finite size effects can influence the accuracy of the

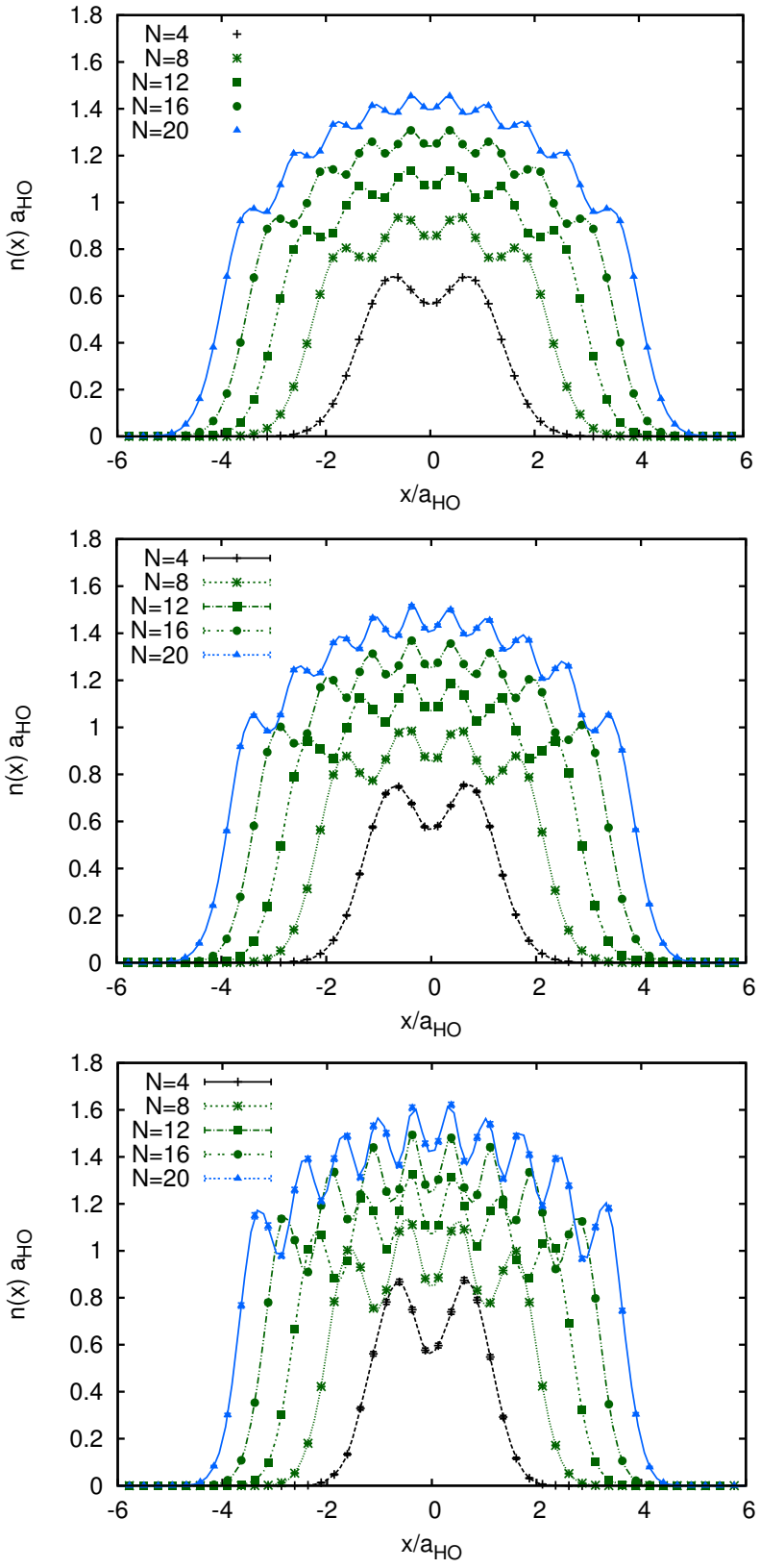

FIG. 9: Density profile of unpolarized, spin-1/2 fermions for several particle numbers $N = 4$, 8, 12, 16, 20. Top: Non-interacting case. Center: $2a_{\rm HO}/a_0 = 1.67$. Bottom: $2a_{\rm HO}/a_0 = 5.16$.

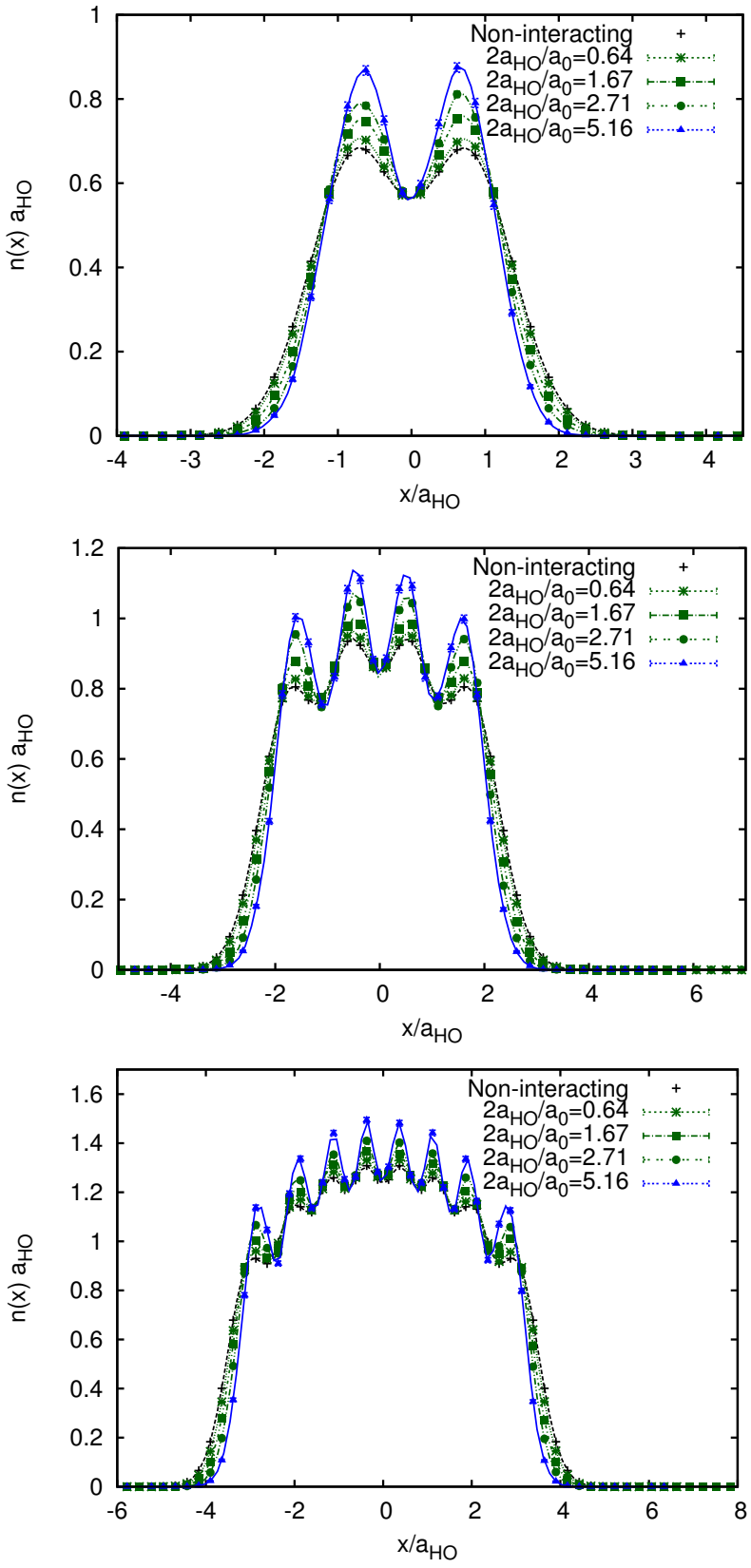

FIG. 10: Density profile of unpolarized, spin-1/2 fermions, for $2a_{\rm HO}/a_0 = 0.64,\ 1.67,\ 2.71,\ 5.16$. Top: $N = 4$. Center: $N = 8$. Bottom: $N = 16$.

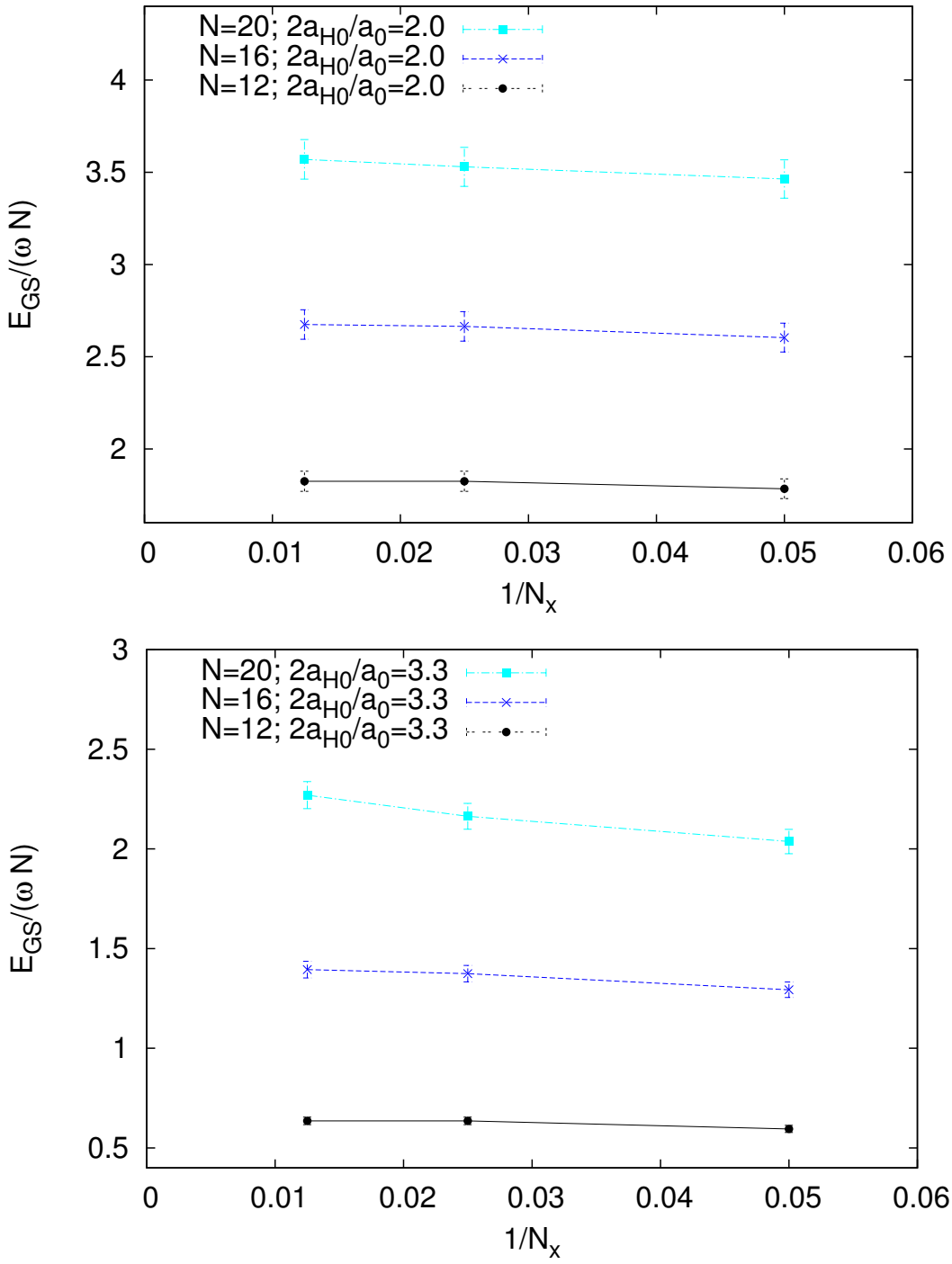

FIG. 11: Top: Lattice-size dependence of the ground-state energy of 12, 16, and 20 unpolarized spin-1/2 fermions, for $N_x = 20, 40, 80$. Top panel: $2a_{\rm HO}/a_0 = 2.0$. Bottom: $2a_{\rm HO}/a_0 = 3.3$. The error bars are purely statistical and show an estimated 3% error for the specific data points shown. Note the change of scale in the energy axes relative to that of the top panel of Fig. 6: the present plots are a zoom-in by a factor of $\simeq 9$.

calculations [7]. In order to see how the size of the lattice affects our calculations, we examine the dependence of the ground-state energy on the lattice size. In Fig. 11 we show the N_x dependence of the ground-state energy per particle at moderate and strong couplings for the largest numbers of particles studied here.

The figures show that the dependence on the lattice size is essentially constant at the moderate coupling, but does show some dependence at stronger coupling. More lattice sizes are required in order to examine the behavior of this dependence, but a naive linear extrapolation shows dependence on the order of 10% for the most strongly coupled system. This represents an upper bound on the systematic error of the dataset evaluated in this project, and most data points show much smaller error, as can be seen in Fig. 6.

Our lattice contains both a spatial and a temporal dimension, as discussed in the methods section. This is another potential source of error in our data. Figure 12 shows the temporal lattice spacing dependence of the energy per particle for $N = 4, 8, 12$ fermions.

The effects induced by a finite temporal lattice spacing are negligible on the scale studied here, and the smoothness of the curves at varied τ (for fixed particle number can be attributed to the success of the renormalization prescription. For each value of τ the coupling is tuned to the physics of the two-body problem, thus absorbing small-τ effects into the renormalization procedure. If our renormalization procedure did not absorb these effects, we would expect to see a splitting in the lines for different τ, just as we do at the strongest couplings for different N_x in Fig. 6. The effects due to finite N_x studied above are much larger than this, as they are clearly discernible on essentially the same scale (see Fig. 6).

The virial theorem, which the energy (both ground state and excited states) and contact must obey, can be written as follows:

$$\langle \hat{H} \rangle = 2\langle \hat{V}_{\text{ext}} \rangle + \frac{1}{2a_0} \frac{\partial \langle \hat{H} \rangle}{\partial (1/a_0)}. \tag{25}$$

Using the definition of the contact as a derivative of the coupling (as in Eq. 24), the virial theorem can be rewritten as

$$\frac{E_{\text{GS}}}{\hbar\omega N} = 2\frac{\langle \hat{V}_{\text{ext}} \rangle}{\hbar\omega N} - \frac{1}{2}\frac{a_0}{2a_{\text{HO}}}\frac{\mathcal{C}a_{\text{HO}}^3}{N}. \tag{26}$$

Another way to check the accuracy of our findings is to compare our results to the virial theorem. As seen in Fig. 13, the virial theorem is satified better at weak coupling than at strong coupling. Although this violation is not very large, there is room for improvement.

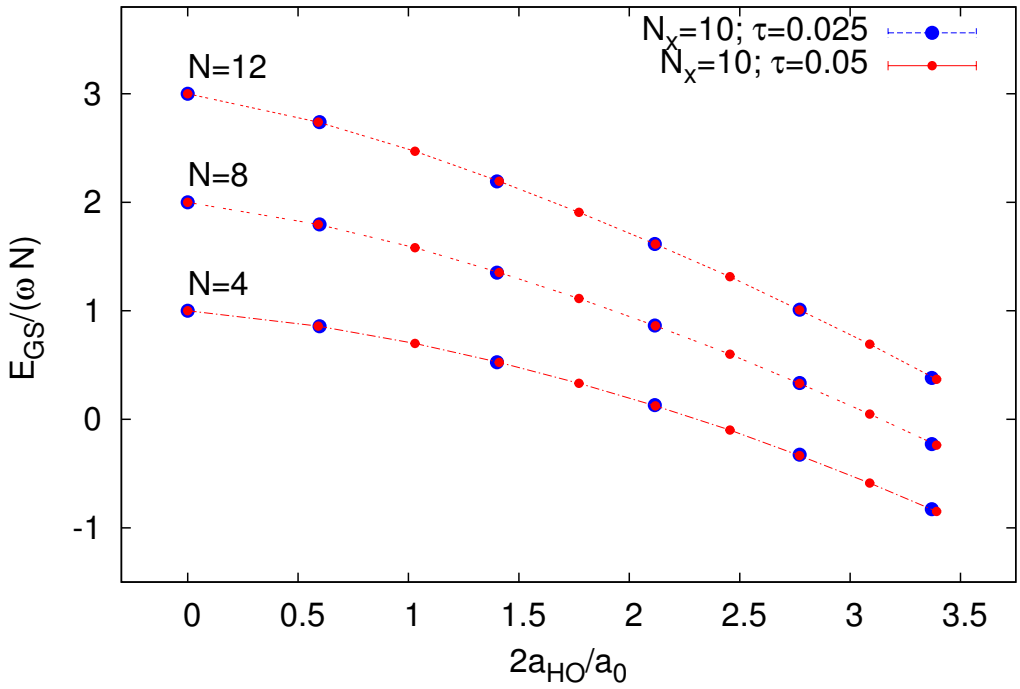

FIG. 12: Temporal lattice spacing (τ) dependence of the ground-state energy of unpolarized spin-1/2 fermions on a $N_x = 10$ non-uniform lattice, for several values of the coupling $2a_{\rm HO}/a_0$, and for several particle numbers. The smoothness of the curves upon reducing τ by a factor of 2 shows that these effects are extremely small (see text for further details).

In particular, the way the contact was determined, based on a numerical derivative of EGS, introduces large uncertainties (not displayed in the figure) that are likely responsible for the differences observed.

V. OUTLOOK

A. Higher Dimensions

The one-dimensional case if interacting trapped fermions has been of great interest in both theory and experiment over the previous few years, but there is also potential to learn a great deal about this system in higher dimensions. We seek to use NFFTs to expand both to higher-dimensional systems and a variety of other potentials. The scaling cost of increasing to two- or three-dimensional cases is enormous, but NFFT algorithms exist which can reduce the scaling and make examination of these cases feasible [10][9].

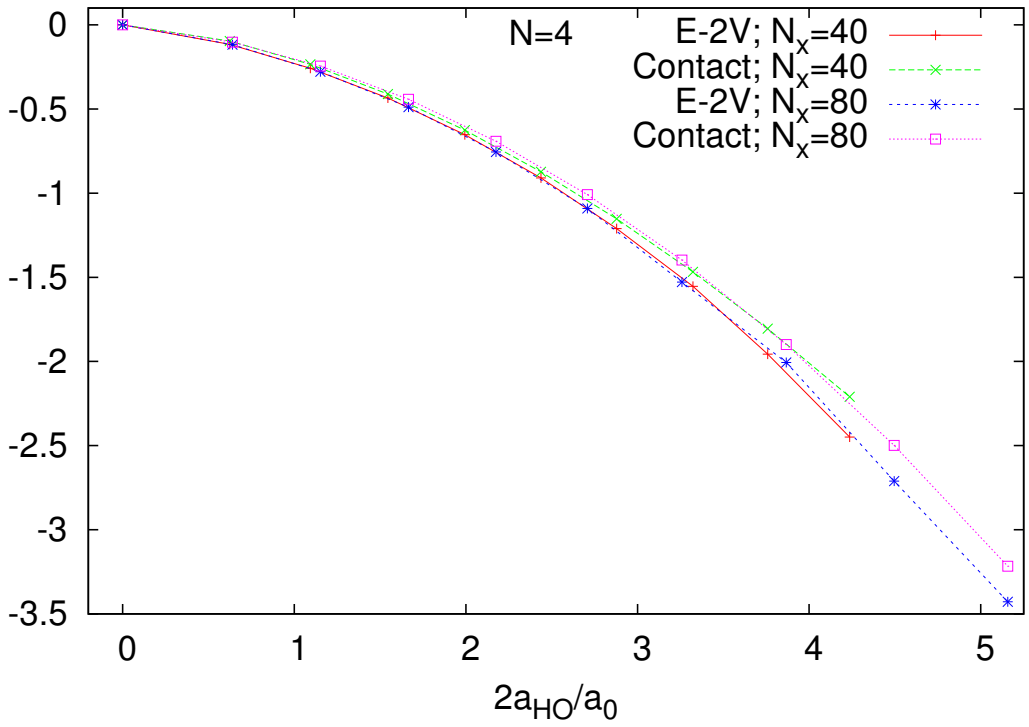

FIG. 13: Δ for a lattice of $N_x = 80$ sites, for $N = 4, 8$,and12 particles.

We have begun to take data for the three-dimensional case, for small lattice sizes due to the increased computational cost. Work has begun to renormalize the three-dimensional case to the known, analytical solution in Ref. [1]. Once the proper renormalization equation is found and the method has been accelerated using the proper fast polynomial transforms, we will be able to examine this system in three dimensions and produce results.

B. Multiple Flavors

This project has focused on two-component fermions, but the method can easily be applied to any number of spin states, as long as there are an even number. Odd numbers of spin states generate a sign problem in the quantum Monte Carlo calculation. The sign problem is one of the major unsolved problems in many-body quantum mechanics, and while there are many current attempts to resolve this problem, we will not attempt to treat it in this work.

Jobs are running to look at this system with $N_f = 4, 6$, and 8. Data analysis is forthcoming.

C. Finite Temperature

Thus far, we have only examined the system at zero temperature. It would be constructive to apply this method to systems at finite temperature. Work has begun on looking at this system at finite temperature.

VI. SUMMARY AND CONCLUSIONS

We have presented a lattice Monte Carlo determination of the ground-state energy, Tan's contact, and density profiles of 1D unpolarized spin-1/2 attractively interacting fermions in a harmonic trap. We have studied systems of up to $N = 20$ particles and performed our calculations by implementing the hybrid Monte Carlo algorithm on a non-uniform Gauss-Hermite lattice, using lattice sizes ranging from $N_x = 10 - 80$. This discretization is a natural basis for systems in an external HO potential, and it yields a position-dependent coupling constant and HS transform. To our knowledge, this is the first attempt to implement such an algorithm. Note that nothing prevents our approach from being generalized to finite temperature and to other interactions, although it would suffer from a sign problem in the same situations as conventional uniform-lattice approaches. It can also be generalized to other external potentials.

Despite the apparent simplicity of the system (only one spatial dimension, only an attractive contact interaction), the ground-state energy and contact were previously unknown, or at least unpublished, and therefore our results are both a benchmark and a prediction for experiments. The same is true of the density profiles reported here. It should be emphasized that our approach to this problem is *ab initio* and exact, up to statistical and systematic uncertainties, both of which we have addressed: the former by taking up to 10^4 de-correlated samples, and the latter by computing for multiple lattice sizes $N_x = 10, 20, 40, 80$.

This work paves the road for future, higher-dimensional studies that will combine non-uniform lattices with non-uniform fast-Fourier transforms as acceleration algorithms [10**?**]. As mentioned above, the latter would enable $O(V \ln^2 V)$ scaling of matrix-vector operations, which is essential for practical calculations in 3D. To our knowledge, NFFT acceleration has never been used in quantum Monte Carlo. Additionally, this work will be expanded to both finite temperature and $N_f > 2$ spin flavors. The spin studies are limited to only

even numbers of spin flavors, as odd numbers generate a sign problem in the Monte Carlo algorithm.

VII. ACKNOWLEDGEMENTS

This thesis began as a summer REU at UNC Chapel Hill. I would like to thank my UNC advisor, Dr. Joaquín Drut, for his constant support and encouragement. In addition, thanks to Jay Porter for useful discussions and comments on the manuscript submitted to Physical Review A.

Many thanks go to Dr. Furnstahl at OSU for facilitating this collaboration with UNC, and for the time and effort put into reviewing this thesis and providing suggestions and resources. Thanks also to Dr. Perry at OSU for his mentorship and support.

This material is based upon work supported by the National Science Foundation Nuclear Theory Program under Grant No. PHY1306520 and National Science Foundation REU Program under Grant No. ACI1156614.

Appendices

A. ANALYTICAL SOLUTIONS

For both solutions, all work is done in first quantization.

The Non-Interacting Case

For non-interacting fermions in a harmonic trapping potential, the Hamiltonian reduces to a sum of single-particle Hamiltonians:

$$\hat{H} = \sum_{i=0}^{\infty} \left(\frac{p_i^2}{2m} + \frac{1}{2} m\omega^2 x_i^2 \right). \tag{27}$$

This sum is independent - each particle, labeled i, can be solved for individually, as there is no interaction between the particles. To find the energy eigenstates of these fermions, we solve the Schrödinger equation:

$$\hat{H}|\psi\rangle = E|\psi\rangle \tag{28}$$

in Dirac notation. Plugging in our Hamiltonian and using units where $\hbar = \omega = m = 1$, this becomes

$$\left(-\frac{1}{2}\frac{d^2}{dx_i^2} + \frac{1}{2}x_i^2 \right) \psi(x_i) = E_i \psi(x_i). \tag{29}$$

in coordinate space, which can be rearranged as follows:

$$\frac{d^2}{dx_i^2} + (x_i^2 - 2E_i)\psi(x_i) = 0. \tag{30}$$

This is the Hermite differential equation. At $x \to \pm\infty$, the harmonic potential goes to infinity, so our wave function, ψ, must go to zero. The solution to this equation (with the boundary conditions $\psi(x \to \pm\infty) = 0$) is a Gaussian times a set of polynomials called the Hermite polynomials:

$$H_n(x_i) = (-1)^n e^{x_i^2} \frac{d^n}{dx_i^n} e^{-x^2}, \tag{31}$$

and the corresponding values of the energy, E are $E_n = n + \frac{1}{2}$, where $n = 0, 1, ...$ are the energy levels. The ground state of a system of N noninteracting fermions in a lattice will consist of the fermions filling the lowest N energy states.

The Interacting, Two-Body Problem

The Hamiltonian for two fermions in a harmonic trap with contact interaction of strength g is as follows:

$$\hat{H} = \frac{1}{2}p_1^2 + \frac{1}{2}x_1^2 + \frac{1}{2}p_2^2 + \frac{1}{2}x_2^2 + g\delta(x_2 - x_1) \tag{32}$$

again using units where $\hbar = \omega = m = 1$. This can be rewritten using relative coordinates: $R = \frac{1}{2}(x_1 + x_2)$ and $r = (x_2 - x_1)$:

$$\hat{H}_{CM} = -\frac{1}{2}\frac{\partial^2}{\partial R^2} + \frac{1}{2}R^2 \tag{33}$$

and

$$\hat{H}_{rel} = -\frac{\partial^2}{\partial r^2} + \frac{1}{4}r^2 + g\delta(r). \tag{34}$$

The center of mass Hamiltonian simply gives us the harmonic oscillator eigensystem, but the relative motion Hamiltonian can be solved separately and the solution added to the harmonic oscillator system. The process in 3D and the results for both 3D and 1D are shown in Ref. [1].

B. DENSITY FUNCTIONAL THEORIES

Density Functional Theories (DFTs) are computational methods that use functionals of the particle densities to determine other important quantum mechanical properties [20],[21]. Density functional theory has been used to study superconductivity, relativistic effects in atomic nuclei, classical liquids, magnetic properties of alloys, and more. DFT is a versatile tool.

The wavefunction, ψ, of a system contains all the information about the system. DFT mainly concerns itself with electronic structure [21], so all particles described here will be fermions, and specifically electrons. Nuclear degrees of freedom (i.e. the lattice in the case of a solid) appear as part of a potential, $V(r)$. This means that the wave function depends only on the coordinates of the electrons, and not the nuclei. Since most of these systems are predominantly non-relativistic, we can write the Schrödinger equation for a single electron as follows:

$$\left[-\frac{\hbar^2 \bigtriangledown^2}{2m} + V(r)\right]\psi(r) = \epsilon\psi(r). \tag{35}$$

For the many-body case (N electrons), the Schrödinger equation as

$$\left[\sum_{i}^{N}\left(-\frac{\hbar^2\bigtriangledown_i^2}{2m}+V(r_i)\right)+\sum_{i<j}U(r_i,r_j)\right]\psi(r_1,r_2,...r_N))=E\psi(r_1,r_2,...r_N)), \tag{36}$$

where $U(r_i, r_j)$ is the interaction potential.

Generally, the approach to quantum mechanical systems is to plug in the potential into the Schrödinger equation, solve for the wave functions, and then take an expectation value of the observable. One such observable is the particle density $n(r)$:

$$n(r)=N\int d^3r_2\int d^3r_3...\int d^3r_N\psi^*(r,r_2,r_3,...r_N))\psi(r,r_2,r_3,...r_N)). \tag{37}$$

Solving the quantum many-body problem in this way is problematic - it is computationally far too burdensome. It quickly becomes impossible to compute solutions for large numbers of particles and complex systems, which eliminates most of the most interesting and relevant problems in physics.

DFT is an alternative to this traditional method of solving for the observables of quantum mechanical systems. While DFT is less accurate, it is more versatile than the Schrödinger's equation. By using the density as a key variable in the problem, it is able to map the many-body problem into what is effectively a one-body problem.

The central premise is that the wave function is far too complicated for many-body systems to manipulate, even with an excellent supercomputer. For $N = 100$ particles in 3D, the wave function of the system contains 300 spatial and 100 spin variables. DFT seeks to solve the system by focusing on a less complicated entity to manipulate. This entity is the Green's function.

One of the limiting cases of the Green's function is called the single-particle density matrix. A further limiting case of that is the particle density, $n(r)$. Information is lost when looking at these limiting cases, but it turns out that it is not lost for the ground state density, $n_0(r)$, because the ground state wave function ψ_0 is completely determined by the ground state density n_0. This is an exact mapping of a many-body problem (that of the ground state wavefunction of N particles) to a few body problem (a funciton of the particle density - i.e. a functional because it is a function of a function).

The density functional formalism was orginally derived by Hohenberg and Kohn in 1964. A more general derivation by Levy followed in 1979. It states that, given a ground-state density $n_0(r)$, it is possible to calculate the corresponding ground-state wavefunction, ψ_0.

This is because the ground-state density contains a second piece of information - it is the density for the lowest energy solution to the N-particle Schrödinger equation [20].

For N fermions (electrons in this case) in an external potential $V_{\text{ext}}(r)$, the Hamiltonian is:

$$H = T + V_{\text{int}} + \sum_{i=1}^{N} V_{\text{ext}}(r_i), \tag{38}$$

where T is the kinetic energy operator and V_{int} is the interaction operator.

Next, a functional is defined for antisymmetric (fermionic) wavefunctions ψ:

$$F[n] = \min_{\psi->n} \langle \psi | T + V_{\text{int}} | \psi \rangle, \tag{39}$$

where the minimum is taken over all ψ that give the density n. A wavefunction that minimizes the functional is denoted by $\psi^n_{min}(r)$. The ground state wavefunction is $\psi^{GS}_{min}(r)$, and we have the ground state energy, E_{GS}, defined as

$$E_{\text{GS}} = \int dr V_{\text{ext}}(r) n_{\text{GS}}(r) + \langle \psi^{GS}_{min} | T + V_{\text{int}} | \psi^{GS}_{min}(r) \rangle = \int dr V_{\text{ext}}(r) n_{\text{GS}}(r) + F[n_{\text{GS}}]. \tag{40}$$

Note that if the ground state is not degenerate, $\psi^{GS}_{min}(r)$ is the only ground state wavefunction. If it is degenerate, $\psi^{GS}_{min}(r)$ is one of the ground state wavefunctions, and the others can be obtained as well.

In principle, using this method, we should be able to calculate all observables [21], but in practice, knowledge of how to compute each observable is not always available. Additionally, the minimization of $E_\nu[n]$ is not trivial, and approximations for $T[n]$ and $U[n]$ may not always be available or reliable. There are various methods for arriving at these approximations, including the Local Density Approximation (LDA), shown in Eq. 2.

C. SUZUKI-TROTTER DECOMPOSITION

When you have a Hamiltonian, H, which is the sum of two or more commuting operators, A_i, you can apply the following identity:

$$e^{\sum_{i=1}^{n} A_i} = \prod_{i=1}^{n} e^{A_i}. \tag{41}$$

However, if these operators do not commute, this identity is no longer true. In numerical simulations, it is much easier to compute the exponential of an operator than the operator itself, so a method must be used to treat these operators as though they commute.

In order to treat non-commuting matrices, we can use the Suzuki-Trotter expansion. In numerical simulations of one-dimensional many-body quantum mechanical systems, the Suzuki-Trotter expansion is used to reduce computational cost. For a set of n operators, $\hat{A}_i$, which may or may not commute with each other:

$$e^{\sum_{i=1}^{n} A_i} = \lim_{m\to\infty} (\prod_{i=1}^{n} e^{A_i/m})^m. \tag{42}$$

For two matrices, for example the two non-commuting portions of our Hamiltonian, $H = H_{\text{HO}} + V_{\text{int}}$, this can be written to second order as:

$$e^{-(H_{\text{HO}}+V_{\text{int}})} = \lim_{m\to\infty} (e^{-H_{\text{HO}}/2m} e^{-V_{\text{int}}/m} e^{-H_{\text{HO}}/2m})^m. \tag{43}$$

This can be applied in quantum Monte Carlo simulations, where we wish to apply the operator (i.e. in projection Monte Carlo).

D. HUBBARD-STRATONOVICH TRANSFORMATIONS

Two-body interactions can be represented as single particles interacting with a bosonic field. The two-body interactions in QED and QCD can be represented by the mediating photon and gluon fields, respectively, but for systems with contact interactions, the field is an "auxiliary field" introduced by a Hubbard-Stratonovich transformation. This transformation substitutes the two-body interaction operator with a path integral over a field ϕ that couples to a one-body operator.

Let's look first at the specific case of spin-1/2 fermions with a contact interaction,

$$V_{\text{int}} = g \sum_n \psi^\dagger_{n,\uparrow} \psi_{n,\uparrow} \psi^\dagger_{n,\downarrow} \psi_{n,\downarrow} \tag{44}$$

The Hubbard Stratonovich transformation is based on the following: for any point in space-time, $a = \mathbf{n}, \tau$, we can write:

$$e^{b_\tau g \psi^\dagger_{a,\uparrow} \psi_{a,\uparrow} \psi^\dagger_{a,\downarrow} \psi_{a,\downarrow}} = \frac{1}{\sqrt{2\pi}} \int_{-\infty}^{\infty} d\phi e^{-\frac{\phi^2}{2} - \phi\sqrt{b_\tau g}(\psi^\dagger_{a,\uparrow}\psi_{a,\uparrow} + \psi^\dagger_{a,\downarrow}\psi_{a,\downarrow})}, \tag{45}$$

Or, in discrete form:

$$e^{b_\tau g \psi^\dagger_{a,\uparrow} \psi_{a,\uparrow} \psi^\dagger_{a,\downarrow} \psi_{a,\downarrow}} = \frac{1}{2} \sum_{\phi=\pm 1} e^{-\phi\sqrt{b_\tau g}(\psi^\dagger_{a,\uparrow}\psi_{a,\uparrow} + \psi^\dagger_{a,\downarrow}\psi_{a,\downarrow})}. \tag{46}$$

This allows us to trade the complexity of the two-body interaction for the computational cost of summing over auxiliary fields, which we are equipped to do through our Monte Carlo simulations.

E. THE PROJECTION MONTE CARLO METHOD

Projection Monte Carlo method is a type of power method in mathematics. It is an algorithm used to compute the largest eigenvalue and corresponding eigenvector of a system. We can use it here to find our ground state energy. Applying the operator $e^{-\beta\hat{H}}$ to an arbitrary state will cause the Hamiltonian, $\hat{H}$ to act on the eigenstates, thus splitting the state into a sum of eigenstates times a multiplicative factor, as follows:

$$e^{-\beta\hat{H}}|\Omega\rangle = c_0 e^{-\beta E_0}|E_0\rangle + c_1 e^{-\beta E_1}|E_1\rangle + c_2 e^{-\beta E_2}|E_2\rangle + \dots \tag{47}$$

As $\beta \to \infty$, the higher energy states - which have larger E_n in the decreasing exponential multiplying the state - will become suppressed. The smallest energy state, the ground state $E - 0$, will be the only surviving term:

$$e^{-\beta\hat{H}}|\Omega\rangle \to c_0 e^{-\beta E_0}|E_0\rangle. \tag{48}$$

Allowing us to isolate the ground state.

In order to find the ground state energy level, $\langle E_0|\hat{H}|E_0\rangle$, we insert our power method operator into the expectation value:

$$\langle\Omega|\hat{H}e^{-\beta\hat{H}}|\Omega\rangle = \langle\Omega|e^{-\frac{\beta\hat{H}}{2}}\hat{H}e^{-\frac{\beta\hat{H}}{2}}|\Omega\rangle, \tag{49}$$

and insert the sum above for the operator on either side of the Hamiltonian.

F. HYBRID MONTE CARLO

Hybrid Monte Carlo (HMC) was first developed in the field of Lattice QCD. It is based on the generation of a Markov sequence of lattice configurations, which are accepted or rejected based on the Metropolis Algorithm. However, whereas in MCMC the lattice is updated locally, in HMC implements molecular dynamics (MD) to update the lattice globally. This reduces the computational cost per sweep from $NN_\tau V^3$ to $NN_\tau V^2$. Further reduction in computational cost can be achieved with the use of acceleration techniques.

Given the probability, $\mathcal{P}[\phi]$, and its corresponding effective action, $S_{\text{eff}} = -log\mathcal{P}[\phi]$, MD introduces a fictitious gaussian-distributed momentum field, called π. This momentum field modifies the partition function, $\mathcal{Z}$, in a way that has no effect on the dynamics of the system

(it is only a multiplicative constant):

$$\mathcal{Z} = \int \mathcal{D}\phi \mathcal{P}[\phi] \rightarrow \int \mathcal{D}\phi \mathcal{D}\pi \mathcal{P}[\phi, \pi] = \int \mathcal{D}\phi \mathcal{D}\pi e^{-\sum_{n,\tau} \frac{\pi_{n,\tau}^2}{2}} \mathcal{P}[\phi] \tag{50}$$

This can be more succinctly written as

$$\mathcal{Z} = \int \mathcal{D}\phi \mathcal{D}\pi e^{-H_{\mathrm{MD}}}, \tag{51}$$

where

$$H_{\mathrm{MD}} \equiv \sum_{n,\tau} \frac{\pi_{n,\tau}^2}{2} + S_{\mathrm{eff}}[\phi]. \tag{52}$$

Because the variables ϕ and $\pi$are not coupled, they are statistically independent. And since the dynamics have not been altered aside from a multiplicative factor, the new probability $\mathcal{P}[\phi, \pi]$ is physically equivalent to the old one, $\mathcal{P}[\phi]$. We now take Hamilton's equations for the new set of variables, ϕ, π:

$$\dot{\phi}_{n,\tau} = \pi_{n,\tau} \tag{53}$$

$$\dot{\pi}_{n,\tau} = F_{n,\tau} \equiv -\frac{\delta S_{\mathrm{eff}}[\phi]}{\delta \phi_{n,\tau}} \tag{54}$$

but now that we have a gaussian-distributed fictitious momentum and the corresponding Hamilton's equations that make it conjugate to the original variable ϕ. As a result, we have a fictitious energy, H_{MD}, which is conserved.

Since the energy is conserved, the ratio taken in the Metropolis algorithm to determine whether a new configuration is accepted or rejected will always be one (within some error on the integrations done to calculate the energy). This means we evolve to the next acceptable energy configuration.

G. THE ISING MODEL

The results are shown in Fig. 14 for a 2D Ising Model calculation. The algorithm was written and compared with the analytical solution in preparation for the thesis work, as a way to become more familiar with computational methods in statistical mechanics.

The analytical solution for the energy per site for the 2D Ising Model is as follows [22]:

$$\epsilon(T) = -2J \tanh(2\beta J) + \frac{K}{2\pi} \frac{dK}{d\beta} \int_0^{\pi} \frac{\sin^2 \phi}{\Delta(1+\Delta)}, \tag{55}$$

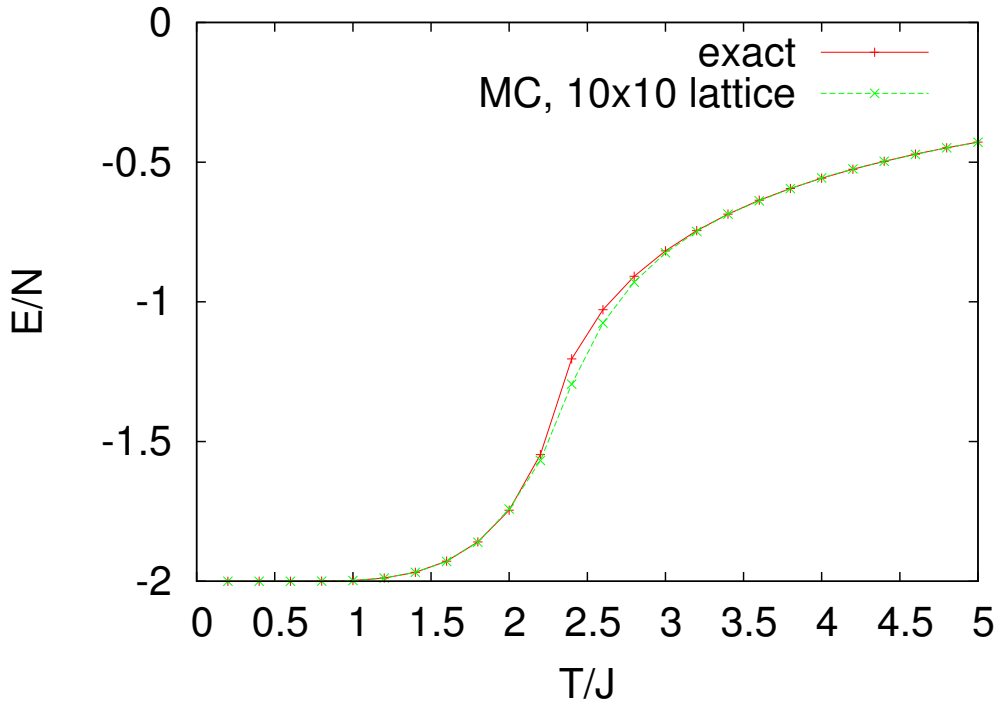

FIG. 14: Results for the energy per site (E/N) as a function of the temperature (scaled to the strength of the coupling) for the 2D Ising Model on a 10×10 lattice. Results compared with the exact solution.

where

$$K = \frac{2}{\cosh(2\beta J \coth(2\beta J)}, \tag{56}$$

and

$$\Delta = \sqrt{1 - K^2 \sin^2 \phi}. \tag{57}$$

This solution was calculated in Mathematica for the same range of temperatures as the computational method. The results in Fig. 14 show that the computational method reproduces the analytical solution exactly at nearly every temperature, except at the critical point, where it shows very small deviations.

[1] Thomas Busch, Berthold-Georg Englert, Kazimierz Rzazewski, and Martin Wilkens. Two cold atoms in a harmonic trap. *Foundations of Physics*, 28(4):549–559, 1998.

[2] Xi-Wen Guan, Murray T. Batchelor, and Chaohong Lee. Fermi gases in one dimension: From bethe ansatz to experiments. *Rev. Mod. Phys.*, 85:1633–1691, Nov 2013.

[3] W. Ketterle and M.W. Zwierlein. Making, probing and understanding ultracold fermi gases. *Ultracold Fermi Gases, Proceedings of the International School of Physics "Enrico Fermi"*, 164:95–287, 2007.

[4] Immanuel Bloch, Jean Dalibard, and Wilhelm Zwerger. Many-body physics with ultracold gases. *Rev. Mod. Phys.*, 80:885–964, Jul 2008.

[5] D. Blume, J. von Stecher, and Chris H. Greene. Universal properties of a trapped two-component fermi gas at unitarity. *Phys. Rev. Lett.*, 99:233201, Dec 2007.

[6] Stefano Giorgini, Lev P. Pitaevskii, and Sandro Stringari. Theory of ultracold atomic fermi gases. *Rev. Mod. Phys.*, 80:1215–1274, Oct 2008.

[7] Joaquín E Drut and Amy N Nicholson. Lattice methods for strongly interacting many-body systems. *Journal of Physics G: Nuclear and Particle Physics*, 40(4):043101, 2013.

[8] Ji-Hong et al Hu. Ground-state properties of the one-dimensional attractive hubbard model with confinement: A comparative study. *Phys. Rev. B*, 82:014202, 2010.

[9] http://www.fftw.org.

[10] Non uniform fast Fourier transform. https://www.nfft.org.

[11] W. Kohn and L. J. Sham. Self-consistent equations including exchange and correlation effects. *Phys. Rev.*, 140:A1133–A1138, Nov 1965.

[12] G. E. Astrakharchik, D. Blume, S. Giorgini, and L. P. Pitaevskii. Interacting fermions in highly elongated harmonic traps. *Phys. Rev. Lett.*, 93:050402, Jul 2004.

[13] Seyed Ebrahim Gharashi, K. M. Daily, and D. Blume. Three s-wave-interacting fermions under anisotropic harmonic confinement: Dimensional crossover of energetics and virial coefficients. *Phys. Rev. A*, 86:042702, Oct 2012.

[14] Shina Tan. Large momentum part of a strongly correlated fermi gas. *Annals of Physics*, 323(12):2971 – 2986, 2008.

[15] Shina Tan. Energetics of a strongly correlated fermi gas. *Annals of Physics*, 323(12):2952 –

2970, 2008.

[16] Shina Tan. Generalized virial theorem and pressure relation for a strongly correlated fermi gas. *Annals of Physics*, 323(12):2987 – 2990, 2008.

[17] S. M. Bhattacharjee and A. Khare. Fifty Years of the Exact Solution of the Two-Dimensional Ising Model by Onsager. *eprint arXiv:cond-mat/9511003*, November 1995.

[18] J. Kotze. Introduction to Monte Carlo methods for an Ising Model of a Ferromagnet. *ArXiv e-prints*, March 2008.

[19] W.H Press et al. *Numerical Recipes in FORTRAN*. Cambridge University Press, 2nd edition, 1992.

[20] R. O. Jones and O. Gunnarsson. The density functional formalism, its applications and prospects. *Rev. Mod. Phys.*, 61:689–746, Jul 1989.

[21] K. Capelle. A bird's-eye view of density-functional theory. *eprint arXiv:cond-mat/0211443*, November 2002.

[22] Mark Tuckerman. Exact solutions of the ising model in 1 and 2 dimensions, May 1999.